Peculiarities of Dansyl Amino Acid Enantioselectivity Using Human Serum Albumin as a Chiral Selector

Eric Peyrin, Yves Claude Guillaume*, and **Christiane Guinchard**
Laboratoire de Chimie Analytique, Faculté de Médecine et Pharmacie, Place St. Jacques, 25030 Besancon Cedex, France

Abstract

This paper describes a novel approach to the study of enantioselectivity variations in a series of apolar D,L-dansyl amino acids with mobile phase pH and temperature on a human serum albumin (HSA) column. The obtained measurement selectivity data are investigated using a new chiral recognition model. This model is based on the formation of complexes between the solute molecule and the binding cavity of the HSA. The thermodynamic results are used to predict a difference in the enantioselectivity mechanism when the side-chain of an asymmetric carbon atom of dansyl amino acids (*R* group) is aliphatic or aromatic. It appears that the steric bulkiness and polarizability of this group are important parameters in the chiral recognition mechanism.

Introduction

Stereoisomeric separation is an important analytical problem, especially in the pharmaceutical industry. Over the past decade, many high-performance liquid chromatographic (HPLC) chiral stationary phases have been developed to separate enantiomers. Separations can be understood through a number of different mechanisms. The major mechanisms are ligand-exchange, π–π interaction, and interaction with chiral polymers. Enantioselective macromolecules include synthetic polymers (polyacrylamides), polysaccharides (cyclodextrins), and proteins. Commercially available protein-bonded phase chiral columns have been made with human α_1-acid glycoprotein (AGP) (1), ovomucoid (OM) (2), bovine serum albumin (BSA) (3), and human serum albumin (HSA) (4). Chiral separation based on inclusion is achieved through a mechanism by which the guest molecule is included in the cavity of a host molecule such as HSA.

Sudlow has characterized two specific binding sites on HSA that are designated site I (or the warfarin site) and site II (or the benzodiazepine site) (5). The three-dimensional structure of HSA has been determined crystallographically (6). Binding sites I and II are located in hydrophobic cavities in subdomains II_A and III_A, respectively, which exhibit similar chemistry (6). The nonpolar residues are sequestered into the hydrophobic cavities inside the protein core, and the polar residues are sequestered onto the surface. The cavity exterior possesses functional groups that act as steric barriers or interact with the guest molecule in a way that induces enantioselectivity. Many previous investigations of ligand-binding to HSA have been reported. These studies have been based on a variety of experimental techniques including equilibrium dialysis, fluorescence, and circular dichroism. The structural requirements for drug-binding to HSA (7) suggest that molecules that bind to the warfarin site are bulky heterocyclic molecules with a negative or positive charge localized in the middle of the molecule (e.g., azapropazone, phenylbutazone, and indomethacin). On the other hand, the benzodiazepine site preferentially binds aromatic carboxylic acids with a generally extended shape, carrying the negative charge on a carboxyl group at one end of the molecule away from the hydrophobic center (e.g., flufenamic acid and fenbufen). Depending on the side-chain, the L-dansyl amino acids bind to either site I or site II. The L-dansyl amino acids specific to site II have a neutral and apolar amino acid side-chain (e.g., L-dansyl tryptophan and L-dansyl norvaline) (7). The L-dansyl amino acids that bind to site I generally have hydrophilic and/or charged substituents on the amino acid side-chain (e.g., L-dansyl arginine and L-dansyl glutamic acid) (7).

Few studies have investigated HSA–solute binding using HPLC. Loun and Hage (8) have characterized the thermodynamic processes involved in the binding and separation of (*R*)- and (*S*)-warfarin on an HSA column by frontal analysis. The effects of temperature on HSA–solute interactions have been studied by Tillelbach (9).

This paper presents the results of an investigation into the mechanistic basis of the stereospecific binding of apolar dansyl amino acids to the HSA chiral column. A simple model of chiral recognition is proposed, and the effects of mobile phase pH and temperature on enantiomeric separation are examined. Gibbs–Helmholtz parameters for chiral discrimination are obtained from ln α-versus-$1/T$ plots. The change in $\Delta(\Delta H)$, $\Delta(\Delta S)$, and $\Delta(\Delta G)$ as a function of the mobile phase pH are discussed for aliphatic and aromatic dansyl amino acids.

* Author to whom correspondence should be addressed.

Model

A simple two-step model of ligand–protein interaction is proposed. The guest molecule approaches the cavity by mutual penetration of the hydration layers (this step is driven by the hydrophobic effect). In the second step, which is responsible for chiral recognition, the solute binds to the nonpolar interior of the binding pocket through a variety of short-range interactions.

Hydrophobic effect

The hydrophobic effect determined the elution order of dansyl amino acids. Figure 1 shows the molecular structure of these compounds. The apolar groups (dimethylaminonaphtyl of the dansyl group and *R*) acted as factors governing the degree of solvation of the analyte in the bulk mobile phase. When the *R* group's hydrophobicity increased, the tendency for the analyte to be excluded from the bulk mobile phase and go toward the protein core on the stationary phase increased. Thus, dansyl tryptophan eluted more slowly from the HSA column than dansyl phenylalanine because the hydrophobicity of the indolyl methyl group was greater than that of the benzyl group.

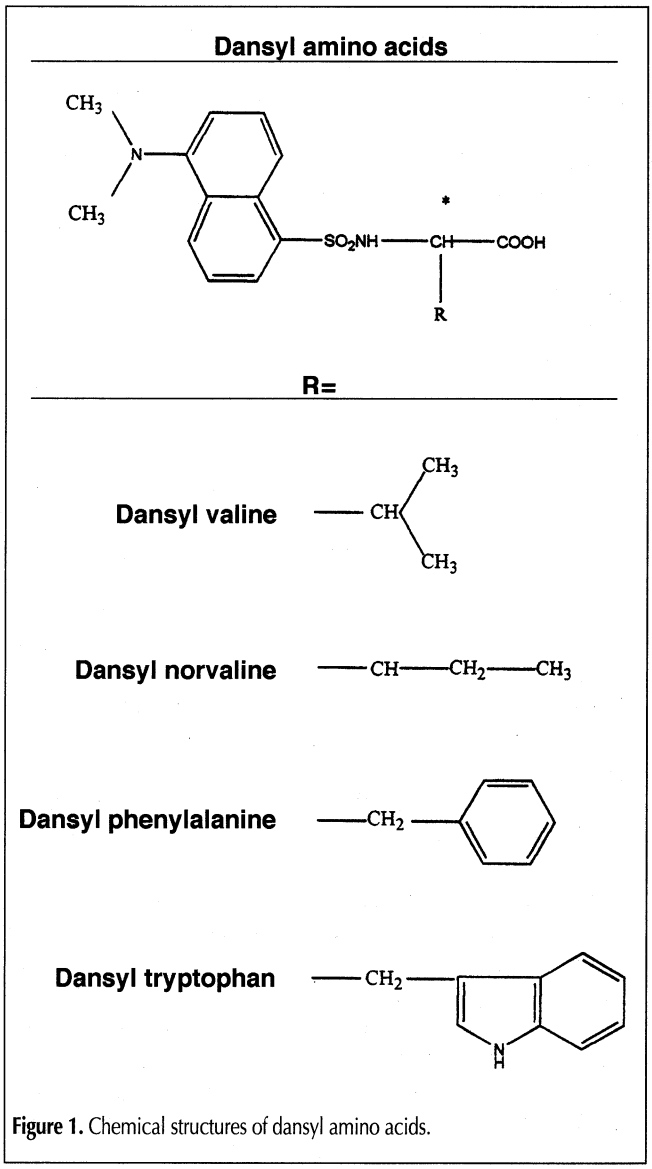

Figure 1. Chemical structures of dansyl amino acids.

Chiral recognition

The HSA–solute short-range interactions consist of a combination of attractive (hydrogen bonding, Van der Waals, electrostatic) and repulsive (steric) interactions (10). Maruyama (11) previously studied the binding of suprofen to site II of HSA using dialysis and spectroscopic techniques. Thermodynamic analysis and proton relaxation rate measurements indicated that the hydrophobic side-chain of suprofen was deeply inserted into the hydrophobic crevice, whereas the carboxyl group interacted with a cationic residue located at or near the surface of HSA. The same behavior was observed for the binding of caprofen to HSA (12,13). Our chiral recognition model for dansyl amino acids was based on a similar binding mode. Specifically, we proposed that the most hydrophobic group (dimethyl amino naphtyl) occupied the interior of the cavity where it was held by Van der Waals interactions. The carboxylate and sulfonylamido groups interacted with cationic and polar residues on the cavity rim by forming electrostatic and hydrogen bonds. The *R* group contributed to the enantioselectivity due to its size, spatial conformation, and polarizability. As can be inferred from Figure 2, binding of the L- enantiomer to site II was destabilized by steric repulsion between the *R* group and the rim of the binding site. In contrast, the D-enantiomer binds more tightly because the *R* group does not contact the rim.

Experimental

Apparatus

The HPLC system consisted of a Merck Hitachi pump L 7100 (Nogent-sur-Marne, France), an Interchim Rheodyne injection valve model 7125 (Montluçon, France) fitted with a 20-µL sample loop, and a Merck L 4500 diode-array detector. The detection wavelength was 254 nm for the solutes and dead time marker. An HSA column (150 × 4.6 mm) supplied by Shandon HPLC (Cergy-Pontoise, France) was used with controlled temperature in an Interchim Crococil TM N°701. After each utilization, the column was stored at 4°C until further use. The mobile phase flow rate was kept at 1 mL/min.

Materials

HPLC-grade acetonitrile (Merck) was used without further purification. Sodium hydrogenphosphate and sodium dihydrogenphosphate were supplied by Prolabo (Paris, France). Water was obtained from an Elgastat option water purification system (Odil, Talant, France) fitted with a reverse-osmosis cartridge. L- and D,L-dansyl valine, L- and D,L-dansyl norvaline, L- and D,L-dansyl phenylalanine, and L- and D,L-dansyl tryptophan were obtained from Sigma Aldrich (Saint Quentin, France). Fresh samples were prepared daily at a concentration of 20 mg/L in acetonitrile. Sodium nitrate at a concentration equal to 0.05M was used as a dead-time marker (Merck). The mobile phase consisted of a 15:85 (v/v) mixture of acetonitrile and 0.05M sodium phosphate buffer adjusted to one of the following pH values: 5.5, 6.0, 6.5, 7.0, 7.5, or 8.0. Each mobile phase was allowed to stand at ambient temperature, and its pH was measured after standing for 1, 2, and 4 h. No pH fluctuations were observed, and the pH

of each mobile phase was within 0.5% of the desired value. Each solute (or a suitable mixture) was injected in 20-µL amounts, and the retention times were measured.

Temperature studies

Retention times were determined over the temperature range of 0–35°C. Each time the temperature was changed, the chromatographic system was allowed to equilibrate for at least 1 h prior to sample injection. To ensure system equilibration, the retention time of D-dansyl valine was measured after 22, 23, and 24 h. The maximum relative difference in the retention time of this compound was never greater than 0.8%, thus demonstrating that the chromatographic system was sufficiently equilibrated for use after 1 h. All the solutes were injected three times at each temperature and pH. Once the measurements were completed at the maximum temperature, the column was immediately cooled to ambient temperature to minimize the possibility of any denaturation of the immobilized HSA.

Thermodynamic relationships

Solute retention is usually expressed in terms of the retention factor (k') by the following well-known equations (14):

$$\ln k' = -\Delta H^0/RT + \Delta S^{0*} \quad \text{Eq 1}$$

$$\Delta S^{0*} = \Delta S^0/R + \ln \phi \quad \text{Eq 2}$$

where ΔH^0 and ΔS^0 are respectively the enthalpy and entropy of the solute transfer from the mobile to the stationary phase, T is the temperature, R is the gas constant, and ϕ is the phase ratio (the volume of the stationary phase divided by the volume of the mobile phase). Additionally, for a pair of D,L- enantiomers, the separation factor (α) between D- and L- enantiomers is given by Equations 3 and 4:

$$\alpha = k'_D/k'_L \quad \text{Eq 3}$$

$$\ln \alpha = -\Delta(\Delta H)/RT + \Delta(\Delta S)/R \quad \text{Eq 4}$$

$$\Delta(\Delta G) = \Delta(\Delta H) - T\,\Delta(\Delta S) \quad \text{Eq 5}$$

where k'_D and k'_L are the capacity factors of D- and L- enantiomers and $\Delta(\Delta H)$ and $\Delta(\Delta S)$ are respectively the differences in the dissolution enthalpy and entropy between D- and L- enantiomers on the chromatogram. From a plot of ln α versus the reciprocal of

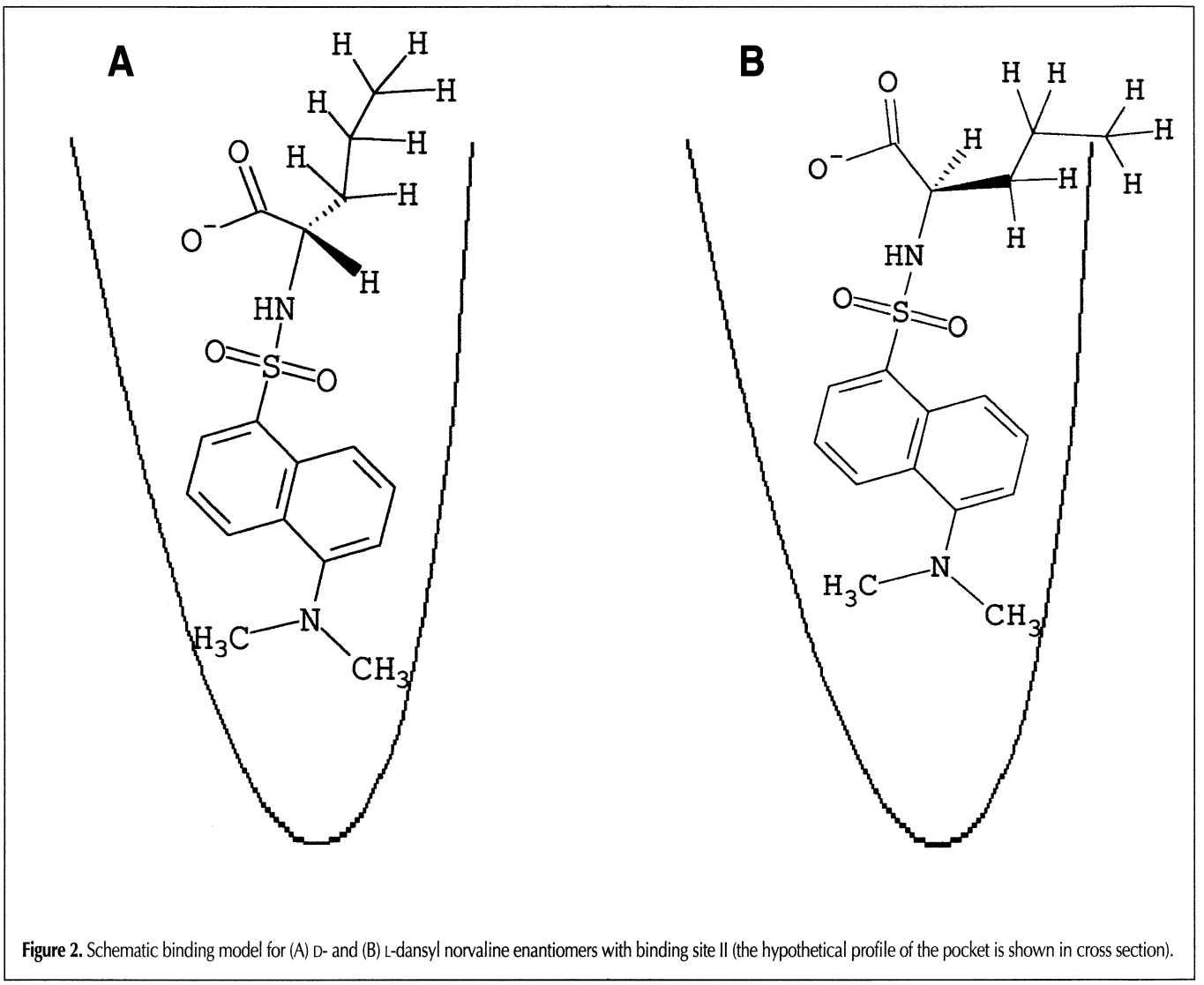

Figure 2. Schematic binding model for (A) D- and (B) L-dansyl norvaline enantiomers with binding site II (the hypothetical profile of the pocket is shown in cross section).

the absolute temperature (called a Van't Hoff plot), Equation 4 allows one to calculate $\Delta(\Delta H)$ and $\Delta(\Delta S)$ from the slope and intercept, respectively. The Gibbs free dissolution energy ($\Delta[\Delta G]$) was determined using Equation 5.

Results and Discussion

Enthalpy–entropy compensation

Investigation of the enthalpy–entropy compensation temperature is a useful thermodynamic approach to the analysis of physicochemical data (14). Mathematically, the compensation enthalpy–entropy can be expressed by the following formula:

$$\Delta G^0_\beta = \Delta H^0 - \beta\Delta S^0 \qquad \text{Eq 6}$$

where ΔG^0_β is the Gibbs free energy of a physicochemical interaction at a compensation temperature β and ΔH^0 and ΔS^0 are the corresponding standard enthalpy and entropy. According to Equation 6, when enthalpy–entropy compensation is observed with a group of compounds in a particular chemical interaction, all the compounds have the same free energy (ΔG^0_β) at temperature β. Therefore, if enthalpy–entropy compensation is observed for the D,L-dansyl amino acids, all of them will have the same retention time at the compensation temperature β, although the temperature dependencies of their retention times may differ. By combining Equations 1, 2, and 6, the following equations were obtained:

$$\ln k'_T = \ln k'_\beta - \Delta H^0/R\,(1/T - 1/\beta) \qquad \text{Eq 7}$$

$$\ln k'_\beta = -\Delta G^0_\beta/(R\beta) + \ln \phi \qquad \text{Eq 8}$$

Equation 7 shows that, if a plot of $\ln k'_T$ against $-\Delta H^0$ is linear, then the D,L-dansyl amino acids are retained by essentially identical interaction mechanisms.

From the Van't Hoff plots of $\ln k'$ versus $1/T$, ΔH^0 values were determined for all of the D- and L-dansyl amino acids at pH 6.0 and 8.0. The correlation coefficients (r) from the plots were greater than 0.98. The typical standard deviations of slope and intercept were 0.005 and 0.03, respectively. For example, the ΔH^0 values of L-dansyl tryptophan were –10.1 and –11.6 kJ/mol at pH 6.0 and 8.0 with standard deviations of 0.2 and 0.3, respectively. The binding of suprofen to HSA site II studied using dialysis was accompanied by a similar negative enthalpy change (11). Plots of

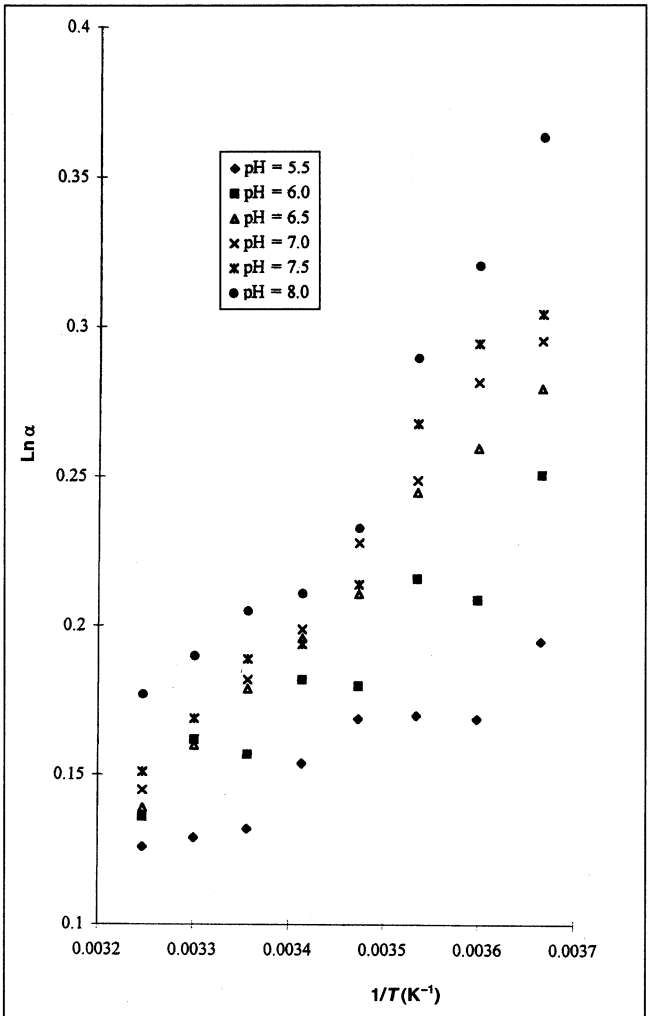

Figure 3. Plots of ln α versus $1/T$ (K^{-1}) for D,L-dansyl norvaline at all mobile phase pH values.

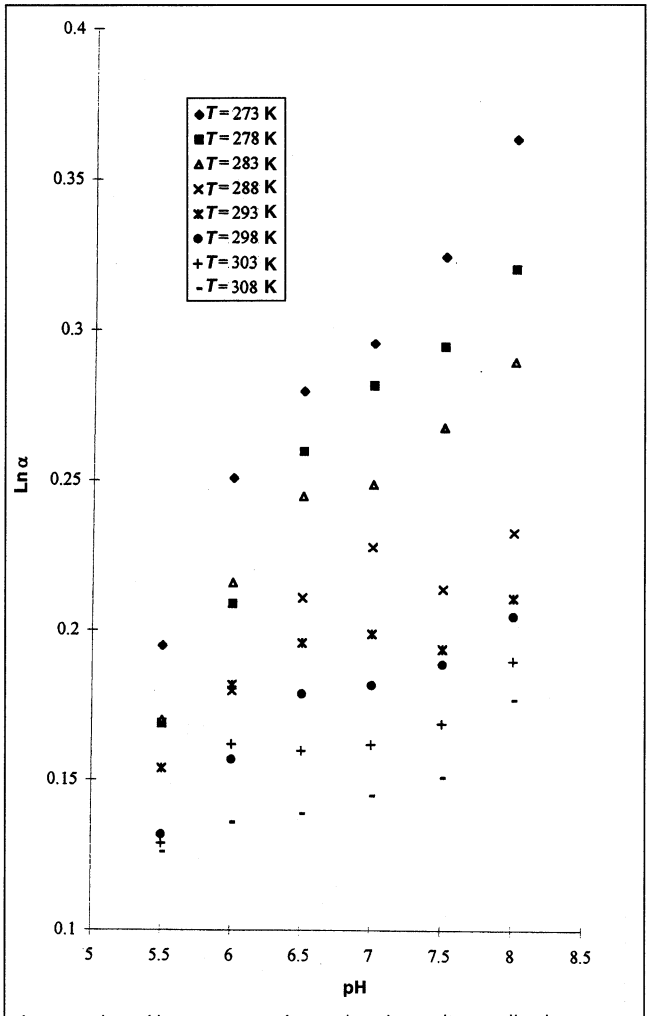

Figure 4. Plots of ln α versus pH for D,L-dansyl norvaline at all column temperature values (T).

ln k'_T (for T = 293 K) calculated for each of the D,L-dansyl amino acids against $-\Delta H^0$ at pH 6 and 8 were drawn. The correlation coefficients for the linear fits were 0.97 and 0.96 for pH 6 and 8, respectively. This can be considered adequate to verify enthalpy–entropy compensation. Thus, it can be concluded that the retention mechanism was independent of the size, structure, and isomeric configuration of the D- and L-dansyl amino acids. This suggested that both enantiomers of each compound studied bound the same location on HSA (i.e., site II). The slope of an enthalpy–entropy compensation can be used to interpret the retention mechanism (15). For a set of compounds in which the enthalpy–entropy compensation exists, the slope will be the same for the same type of reaction (15). The relative difference in the slope values obtained for pH 6.0 and 8.0 was less than 3%, thus indicating that the retention mechanism was the same at both acidic and basic pH.

Table I. Capacity Factors k'_D and k'_L with Standard Deviations and Selectivity* of Dansyl Amino Acid Enantiomers†

Dansyl amino acid	k'_D (SD)	k'_L (SD)	α
Dansyl valine	5.02 (0.01)	4.18 (0.02)	1.15
Dansyl norvaline	6.17 (0.02)	5.14 (0.01)	1.20
Dansyl phenylalanine	12.54 (0.03)	9.72 (0.03)	1.29
Dansyl tryptophan	16.22 (0.04)	13.98 (0.04)	1.16

* $\alpha = k'_D/k'_L$
† pH = 6.0, and T = 293 K.

Enantioselectivity variations

Using Equation 4, Van't Hoff plots for ln α versus $1/T$ were obtained for all D,L-dansyl amino acids at each mobile phase pH (5.5, 6.0, 6.5, 7.0, 7.5, and 8.0). The correlation coefficients for all linear fits were in excess of 0.95. The typical standard deviations of the slope and intercept obtained were 0.006 and 0.03, respectively. Figure 3 shows the Van't Hoff plots for D,L-dansyl norvaline at all the pH values studied. As predicted by our model, dansyl tryptophan was retained more than dansyl phenylalanine, and in all cases, the L-

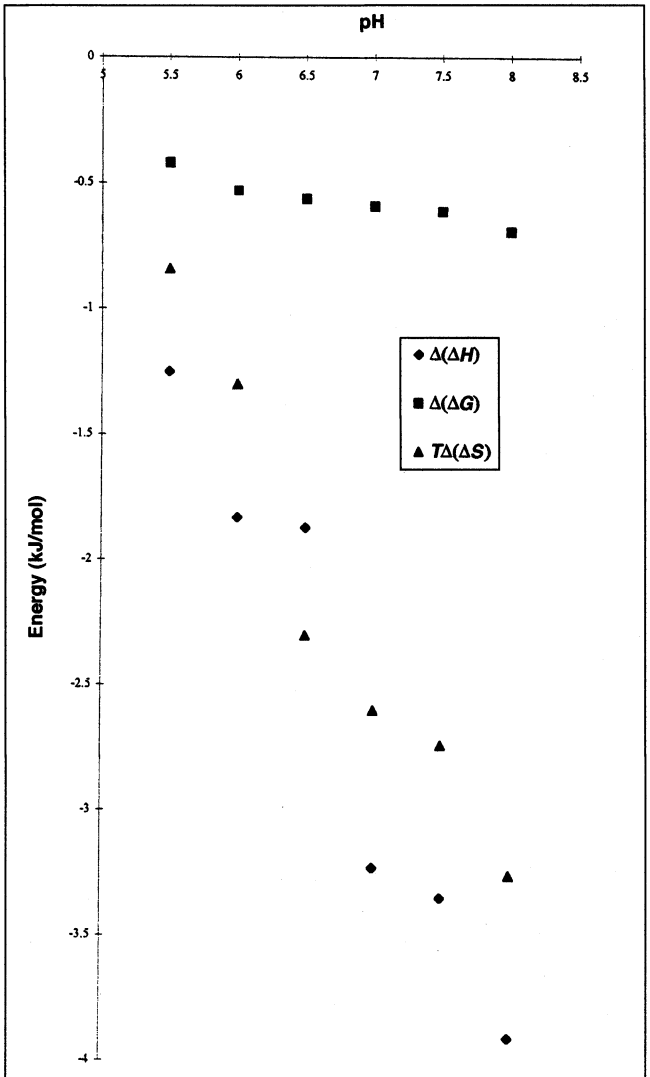

Figure 5. Plots of thermodynamic parameters (kJ/mol) Δ(ΔH), T Δ(ΔS), and Δ(ΔG) versus mobile phase pH for D,L-dansyl norvaline; T = 283 K.

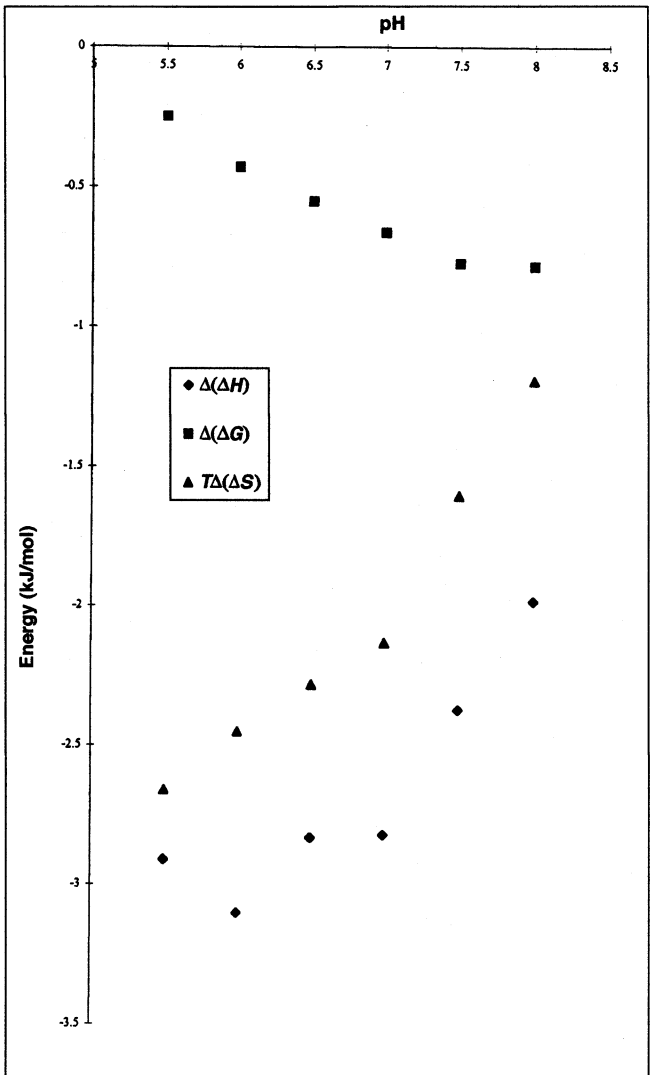

Figure 6. Plots of thermodynamic parameters (kJ/mol) Δ(ΔH), T Δ(ΔS), and Δ(ΔG) versus mobile phase pH for D,L-dansyl tryptophan; T = 283 K.

enantiomer was eluted before the D- enantiomer. Table I shows k' and α values for dansyl amino acids at 20°C and pH 6.0. The plots of ln α versus pH showed linear and increasing variations for all D,L-dansyl amino acids at each column temperature. The correlation coefficients for all linear plots were at least 0.90. Figure 4 shows these linear variations for D,L-dansyl norvaline at different temperatures. To explain the increase in selectivity with pH, Gibbs–Helmholtz parameters were calculated. Table II contains a complete list of $\Delta(\Delta H)$ and $\Delta(\Delta S)$ values for all dansyl amino acids as a function of mobile phase pH. As ln α increased with the pH for all solutes, $\Delta(\Delta G)$ became more negative (Figures 5 and 6).

From the values listed in Table II, the following hypothesis can be drawn. For aliphatic dansyl amino acids (dansyl norvaline and dansyl valine), $\Delta(\Delta H)$ and $\Delta(\Delta S)$ became increasingly negative as the pH increased. The electrostatic attraction between the carboxylate group of the solute and the cationic residue located at or near the cavity rim was diminished as the pH varied from 5.5 to 8.0. At high pH values, this caused a change in the solute conformation in the pocket. Consequently, the aliphatic dansyl amino acids engaged strong stereoselective hydrogen bonding and/or Van der Waals interactions with the rim of the cavity. This would explain the observed trends of $\Delta(\Delta H)$ and $\Delta(\Delta S)$ to decrease when pH increased (Figure 5). Therefore, it can be said that the increase in the enantioselectivity of aliphatic dansyl amino acids at high pH values was controlled enthalpically.

For aromatic dansyl amino acids (dansyl phenylalanine and dansyl tryptophan), $\Delta(\Delta H)$ and $\Delta(\Delta S)$ became smaller negative values as the pH increased. In this case, the side-chains were more highly polarizable than they were for the aliphatic dansyl amino acids. Thus, contrary to the aliphatic dansyl amino acids, the aromatic *R* group did not remain in the bulk solvent. They engaged like the dansyl group with apolar residues in the hydrophobic cavity to nearly the same extent for the D- and L-enantiomers. This caused the lowest chiral recognition due to the smallest difference between the average conformations of the D,L- enantiomeric complexes. This result was confirmed by the weak selectivity values. At pH 5.5, for example, α for dansyl tryptophan was 1.12 at 5°C, 1.07 at 20°C, and 1.00 at 35°C. However, the aromatic *R* group for L- was always nearer to the cavity rim than the D- enantiomer. When the pH increased, the electrostatic interactions between the enantiomer and the cavity rim decreased. Thus, the steric constraints in the cavity between the aromatic *R* and dansyl group for D- were lower than those for the L- enantiomer. Therefore, D- at high pH values increased its affinity for HSA relative to the L- enantiomer by an *R* group with a higher degree of liberty in the cavity. This would explain the trends observed for $\Delta(\Delta H)$ and $\Delta(\Delta S)$ to increase when the pH increased (Figure 6). Therefore, it can be said that the increase in the enantioselectivity of aromatic dansyl amino acids at high pH values was controlled entropically. For dansyl tryptophan, large variations were noted in $\Delta(\Delta H)$ and $\Delta(\Delta S)$ values (Table II). On the other hand, there was little or no change in the $\Delta(\Delta H)$ and $\Delta(\Delta S)$ values for dansyl phenylalanine within the experimental error. This difference can be explained by a weak polarizability and steric bulkiness of its benzyl group in relation to the indolyl methyl group of the dansyl tryptophan.

Conclusion

A description of the enantioselectivity variations in apolar dansyl amino acids on an HSA column showed a behavior difference between aromatic and aliphatic compounds. Enthalpy–entropy compensation revealed that the retention mechanism of these molecules was independent of their molecular structure at acidic and basic pH. A simple model was proposed to understand Gibbs–Helmholtz parameter trends with mobile phase pH and column temperature. It showed the importance of the solute spatial arrangement, *R* group polarizability, and steric interactions at site II of the HSA protein on the chiral recognition mechanism.

Acknowledgments

The authors would like to thank Nadia Morin and Mireille Thomassin for their assistance.

References

1. A.F. Fell, T.A.G. Noctor, J.E. Mama, and B.J. Clark. J. Computer-aided optimization of drug enantiomer separation in chiral high-performance liquid chromatography. *J. Chromatogr.* **434:** 377–84 (1988).
2. B.M. Eriksson and A. Wallin. Evaluation of the liquid-chromatographic resolution of indenoindolic racemic compounds on three protein-based chiral stationary phases. *Pharm. Biomed. Anal.* **13:** 551–61 (1995).
3. R.K. Gilpin, S.E. Ehtesham, and R.B. Gregory. Liquid chromatography studies of the effect of temperature on the chiral recognition of tryptophan by silica immobilized bovine albumin. *Anal. Chem.* **63:** 2825–28 (1991).

Table II. Thermodynamic Parameters $\Delta(\Delta H)$ and $\Delta(\Delta S)$ with Standard Deviations for all Dansyl Amino Acid Enantiomers at Different Mobile Phase pH Values

	pH 5.5		pH 6.0		pH 6.5		pH 7.0		pH 7.5		pH 8.0	
D,L- Enantiomer pair	$\Delta(\Delta H)$	$\Delta(\Delta S)$	$\Delta(\Delta H)$	$\Delta(\Delta S)$	$\Delta(\Delta H)$	$\Delta(\Delta S)$	$\Delta(\Delta H)$	$\Delta(\Delta S)$	$\Delta(\Delta H)$	$\Delta(\Delta S)$	$\Delta(\Delta H)$	$\Delta(\Delta S)$
Dansyl valine	–2.5 (0.1)	–7.7 (0.1)	–2.6 (0.1)	–7.8 (0.1)	–3.0 (0.1)	–8.8 (0.3)	–3.5 (0.1)	– 10.4 (0.1)	–5.3 (0.2)	– 17.0 (0.1)	–5.1 (0.1)	–15.8 (0.1)
Dansyl norvaline	–1.2 (0.1)	–3.0 (0.1)	–1.8 (0.1)	–4.6 (0.1)	–2.9 (0.1)	–8.2 (0.2)	–3.2 (0.1)	–9.3 (0.1)	–3.3 (0.1)	–9.7 (0.1)	–3.9 (0.1)	–11.4 (0.1)
Dansyl phenylalanine	–1.5 (0.1)	–3.1 (0.1)	–1.5 (0.1)	–2.9 (0.1)	–1.4 (0.1)	–2.9 (0.1)	–1.4 (0.1)	–2.8 (0.1)	–1.4 (0.1)	–2.8 (0.1)	–1.4 (0.1)	–2.7 (0.1)
Dansyl tryptophan	–2.9 (0.1)	–9.4 (0.1)	–3.1 (0.1)	–9.3 (0.1)	–2.8 (0.1)	–8.1 (0.2)	–2.8 (0.1)	–7.6 (0.1)	–2.4 (0.1)	–5.6 (0.1)	–2.0 (0.1)	–4.2 (0.3)

4. B. Loun and D.S. Hage. Chiral separation mechanism in protein-based HPLC columns. 2. Kinetic studies of (*R*) and (*S*) warfarin binding to immobilized human serum albumin. *Anal. Chem.* **68:** 1218–25 (1996).
5. G. Sudlow, D.J. Birkett, and D.N. Wade. The characterization of two specific drug binding sites on human serum albumin. *Mol. Pharmacol.* **11:** 824–32 (1975).
6. X.M. He and D.C. Carter. Atomic structure and chemistry of human serum albumin. *Nature* **358:** 209–15 (1992).
7. G. Sudlow, D.J. Birkett, and D.N. Wade. Further characterization of specific drug binding sites on human serum albumin. *Mol. Pharmacol.* **12:** 1052–1061 (1976).
8. B. Loun and D.S. Hage. Chiral separation mechanisms in protein-based HPLC columns. 1. Thermodynamics studies of (*R*) and (*S*) warfarin binding to iramobilized human serum albumin. *Anal. Chem.* **66:** 3814–22 (1994).
9. V. Tillelbach and R.K. Gilpin. Species dependency of the liquid chromatographic properties of silica-immobilized serum albumins. *Anal. Chem.* **67:** 44–47 (1995).
10. A.M. Krstulovic. Chiral stationary phases for the liquid chromatographic separation of pharmaceuticals. *J. Pharm. Biomed Anal.* **6:** 641–58 (1988).
11. T. Maruyama, C.C. Lin, K. Yamasaki, T. Miyoshi, T. Imai, M. Yamasaki, and M. Otagiri. Binding of suprofen to human serum albumin. Role of the suprofen carboxyl group. *Biochem. Pharmacol.* **45:** 1017–26 (1993).
12. M.H. Rahman, T. Maruyama, T. Okada, K. Yamasaki, and M. Otagiri. Study of interaction of carprofen and its enantiomers with human serum albumin. Mechanism of binding studied by dialysis and spectroscopic methods. *Biochem. Pharmacol.* **46:** 1721–31 (1993).
13. H. Kohita, Y. Matsuhita, and I. Moriguchi. Binding of caprofen to human and bovin serum albumins. *Chem. Pharm. Bull.* **42:** 937–40 (1994).
14. Y. Guillaume and C. Guinchard. Retention mechanism of weak polar solutes in reversed phase liquid chromatography. *Anal. Chem.* **68:** 2869–73 (1996).
15. F. P. Tomasella, J. Fett, and L.J. Cline Love. Effect of organic modifier and temperature on micellar liquid chromatography. *Anal. Chem.* **63:** 474–79 (1991).

Manuscript accepted October 8, 1997.